# Chapter 6

# Study of cracked orthotropic elastic strip under normal impact loading conditions

## 6.1 Introduction

With the increased usage of composite materials, the researchers are very much attracted towards the problems of composites. Composite materials are by nature anisotropic. Thus, the study of an anisotropic medium with a crack is of great importance in fracture analysis of composites.

The dynamic problems of singular stresses around cracks in an orthotropic medium are few in number. This may be due to mathematical complexity of such problems. The behaviour of dynamic stress intensity factor on cracked faces subject to normal impact loading was observed by Freund (1974). Kassir and Bandyopadhyay (1983) have considered the elasto-dynamic response of an infinite orthotropic solid containing a crack under the action of impact loading. Itou (1989) studied the dynamic stress intensity factors around two coplanar Griffith cracks in an orthotropic layer sandwiched between two isotropic elastic half planes. Due to the presence of finite boundaries, the problems become more complicated and analytical treatments on the transient crack problems for orthotropic materials including the effect of boundaries are few in number. Gonzalez and Mason (2000) have studied the problem of mixed mode dynamic stress intensity factor subjected to point loading condition. Rizza (2003) studied impact

The contents of this chapter have been communicated in **International Journal of Engineering Sciences.**

response of a cracked orthotropic material. Itou (2010) had studied the dynamic stress intensity factors for two parallel interfacial cracks between a non-homogeneous bonding layer and two dissimilar elastic half planes subjected to an impact loading condition. Composite materials are widely used in engineering applications, so their mechanical behavior becomes important for the fundamental understanding. In composite materials dynamic crack propagation and the response of cracked composite bodies under concentrated point loading condition have been investigated both theoretically and experimentally by researchers few (Shindo et al. (1985, 1999), Ma et al. (2005), Rizza (2003), Hongmin et al. (2007), Freund (1973, 1990)) names working in the field of composite materials.

In isotropic solids many exact solutions exist for the evaluation of stress field around stationary and propagating cracks but in case of anisotropic solids only few solutions are available for the stress field around stationary and propagating cracks. This is due to the mathematical complexity of such problems. Generally integral transform techniques are used to solve problems involving cracked orthotropic bodies subjected to impact loading conditions which leads to a Fredholm integral equation on the Laplace transform domain, rather than a Weiner-Hopf equation as is found for isotropic materials. The dynamic stress intensity factor on the time domain is recovered through numerical inversion of the solution of the Fredholm equation. This process can be numerically challenging and computationally intensive.

Analytic Inversion of the Laplace transform is defined as contour integration in the complex plane. For simple $F(p) = L[f(t)]$, Cauchy's residue theorem can be employed by taking Bromwich contour. For complicated $F(p) = L[f(t)]$, this approach can be too complicated to perform even using symbolic software like Matlab or Mathematica.

There is no single method which works well for all the problems of Laplace inversion. Therefore it is necessary to study another alternative to tackle the problem. Bellman et al. (1966) proposed a numerical method to calculate the inverse Laplace transformation (see Appendix A). Beside this method there are other two methods to evaluate the inverse Laplace transform, first one is using numerical integration while second one is using fast Fourier Transform (FFT) technique algorithm. The comparison of applicability and accuracy among of these three methods was studied by Ueda (1988).

The merit of the method proposed by Bellman et al. (1966) is that only a few values are sufficient for the inverting process. Therefore this method is useful to those problems that require long CPU time to calculate the values in the Laplace transformed domain. In case of numerical integral method and FFT method few parameters are required. But the Numerical integral method takes too much CPU time to calculate the inverting process. In the FFT method there is provision for choosing suitable parameters the choice of suitable parameters. If suitable parameters are obtained, this method can carry out the inversion process in the shortest time as compared to numerical integration method. This method had already been successfully used by Escobar et al. (2014), Sur and Kanoria (2015) and Mukhopadhyay and Kumar (2010), during handling of various physical and scientific problems.

The present chapter deals with the study of an infinite orthotropic elastic strip with a finite crack subject to suddenly applied point load on the cracked surfaces. The problem under normal impact response of an orthotropic medium with a central crack has been investigated. Laplace and Fourier integral transforms are employed to reduce the two dimensional wave propagation problems to the solution of a pair of dual integral equations in the Laplace transformed plane. These integral equations have been reduced

to the solution of a set of integral equations which have further been reduced to the solution of an integro-differential equation. The iteration method has been used to obtain the low frequency solution of the problem. To determine the time dependence of the solution the expressions are inverted to yield the dynamic stress intensity factor and crack opening displacement for normal point force loading. Numerical results of these physical quantities for normal point loading and for a large normalized time variable have been calculated for graphite-epoxy and glass-epoxy composite materials for different particular cases, which have been depicted through graphs.

**6.2 Problem Formulation**

Consider an elaso-dynamic crack problem of a central crack $|x| \le a,\ y = \pm 0$ situated in an orthotropic elastic strip of thickness $2h$ $(-\infty < x < \infty, -h \le y \le h)$, subject to sudden loading. The displacement equations of motion are given as

$$C_{11}\frac{\partial^2 u}{\partial x^2} + \frac{\partial^2 u}{\partial y^2} + (C_{12}+1)\frac{\partial^2 v}{\partial x \partial y} = \frac{1}{C_s^2}\frac{\partial^2 u}{\partial t^2}, \tag{6.1}$$

$$C_{12}\frac{\partial^2 v}{\partial x^2} + \frac{\partial^2 v}{\partial y^2} + (C_{12}+1)\frac{\partial^2 u}{\partial x \partial y} = \frac{1}{C_s^2}\frac{\partial^2 v}{\partial t^2}, \tag{6.2}$$

where $u$, $v$ are the horizontal and vertical displacements respectively, $C_s^2$ is equal to $\mu_{12}/\rho$ with $\mu_{12}$ be the shear modulus, $\rho$ and $C_{ij}$ $(i, j = 1, 2, 3)$ are the density and elastic constants of the material respectively.

In the Laplace transformed plane the field equations become

$$C_{11}\frac{\partial^2 u^*}{\partial x^2} + \frac{\partial^2 u^*}{\partial y^2} + (C_{12}+1)\frac{\partial^2 v^*}{\partial x \partial y} - \frac{p^2 u^*}{C_s^2} = 0, \tag{6.3}$$

$$C_{12}\frac{\partial^2 v^*}{\partial x^2} + \frac{\partial^2 v^*}{\partial y^2} + (C_{12}+1)\frac{\partial^2 u^*}{\partial x \partial y} - \frac{p^2 v^*}{C_s^2} = 0, \tag{6.4}$$

where $u^*$ and $v^*$ are the transformed displacement components and are the functions of $x$, $y$ and $p$. Under the sudden impact loadings applied on surfaces of the crack

guarantees the symmetry requirements of the mathematical model considered in the half strip $0 \le y \le h$. The boundary conditions on $y = 0$ are taken as

$$\sigma_{yy}(x,0,t) = -\sigma_0(x)H(t), \qquad |x| < a, \tag{6.5}$$

$$v(x,0,t) = 0, \qquad |x| \ge a, \tag{6.6}$$

$$\tau_{xy}(x,0,t) = 0, \qquad |x| < \infty, \tag{6.7}$$

and the boundary conditions on $y = h$ are

$$u(x,h,t) = 0, \qquad |x| < \infty, \tag{6.8}$$

$$v(x,h,t) = 0, \qquad |x| < \infty, \tag{6.9}$$

where $\sigma_0(x)$ is the known crack surface traction and $H(t)$ denotes the Heaviside unit step function. It is considered that displacements and stresses are vanished at remote distances from crack. The reduced boundary conditions in the Laplace transformed plane are given as

$$\sigma^*_{yy}(x,0,p) = -\frac{\sigma_0(x)}{p}, \qquad |x| \le a, \tag{6.10}$$

$$v^*(x,0,p) = 0, \qquad |x| \ge a, \tag{6.11}$$

$$\tau^*_{xy}(x,0,p) = 0, \qquad |x| < \infty, \tag{6.12}$$

$$u^*(x,h,p) = 0, \qquad |x| < \infty, \tag{6.13}$$

$$v^*(x,h,p) = 0, \qquad |x| < \infty. \tag{6.14}$$

To obtain the solution of the equations (6.3) and (6.4) subject to the conditions (6.10) - (6.14), assume that the displacements in Laplace transformed domain are of the form

$$u^*(x,y,p) = \int_0^\infty A(s,y,p)\sin(sx)\,ds, \tag{6.15}$$

$$v^*(x,y,p) = \int_0^\infty \frac{1}{s} B(s,y,p)\cos(sx)\,ds, \tag{6.16}$$

where

$$A(s,y,p)=A_1(s,p)ch\gamma_1 y+A_2(s,p)ch\gamma_2 y+C_1(s,p)sh\gamma_1 y+C_2(s,p)sh\gamma_2 y,$$

$$B(s,y,p)=B_1(s,p)sh\gamma_1 y+B_2(s,p)sh\gamma_2 y+D_1(s,p)ch\gamma_1 y+D_2(s,p)ch\gamma_2 y,$$

in which $\gamma_1^2$, $\gamma_2^2$ are the positive roots of the equation

$$C_{22}\gamma^4+\left[\left(C_{12}^2+2C_{12}-C_{11}C_{22}\right)s^2-\left(1+C_{22}\right)\frac{p^2}{C_s^2}\right]\gamma^2+\left(C_{11}s^2+\frac{p^2}{C_s^2}\right)\left(s^2+\frac{p^2}{C_s^2}\right)=0$$

and

$$B_j(s,p)=-\alpha_j A_j(s,p),\ D_j(s,p)=-\alpha_j C_j(s,p),\ \alpha_j(s,p)=\frac{C_{11}s^2+p^2/C_s^2-\gamma_j^2}{(1+C_{12})r_j},\qquad j=1,2.$$

The boundary conditions (6.13) and (6.14) with the aid of equation (6.12) yield

$$A_1(s,p)=\delta_1(s,p)C_1(s,p),$$

$$A_2(s,p)=\delta_2(s,p)C_2(s,p),$$

where the unknown functions $\delta_j(s,p)$, $(j=1,2)$ are given as

$$\delta_1(s,p)=\frac{\frac{\alpha_2\beta_1}{\beta_2}+\alpha_2 sh\gamma_1 h\ sh\gamma_2 h-\alpha_1 ch\gamma_1 h\ ch\gamma_2 h}{\alpha_1 sh\gamma_1 h\ ch\gamma_2 h-\alpha_2 sh\gamma_1 h\ ch\gamma_2 h},$$

$$\delta_2(s,p)=\frac{\alpha_1+\frac{\alpha_1\beta_1}{\beta_2}sh\gamma_1 h\ sh\gamma_2 h-\frac{\alpha_1\beta_1}{\beta_2}ch\gamma_1 h\ ch\gamma_2 h}{\alpha_1 sh\gamma_1 h\ ch\gamma_2 h-\alpha_2 sh\gamma_2 h\ ch\gamma_1 h}.$$

with $\beta_j=\alpha_j+\gamma_j^2,\qquad j=1,2.$

The boundary conditions (6.10) and (6.11) with the aid of above relations give rise to the following pair of dual integral equations

$$\int_0^\infty F(s,p)D(s,p)\cos(sx)ds=-\frac{\sigma_0(x)}{\mu_{12}p},\quad 0<x<a,\tag{6.17}$$

$$\int_0^\infty D(s,p)\cos(sx)ds=0,\quad x\ge a,\tag{6.18}$$

where $D(s,p)=\dfrac{(\alpha_1-\beta\alpha_2)}{s}C_1(s,p)$,

$F(s,p)=\dfrac{\left(C_{12}s^2-C_{22}\alpha_1\gamma_1\right)\delta_1(s)+\left(C_{12}s^2-C_{22}\alpha_2\gamma_2\right)\delta_2(s)}{(\alpha_1-\beta\alpha_2)}$ and $\beta=\dfrac{\beta_1}{\beta_2}$.

### 6.3 Method of Solution

Considering the state of integral equation (6.18) as

$$D(s,p)=\frac{1}{s}\int_0^a f(t,p)\sin(st)dt\,, \tag{6.19}$$

where $f(t,p)$ is an unknown function to be determined.

The equation (6.17) finally reduces to the following singular integral equations as

$$\frac{d}{dx}\int_0^\infty f(t)\log\left|\frac{t+x}{t-x}\right|dt=2\left[\sigma_1(x)-\frac{d}{dx}\int_0^a f(t)dt\int_0^x\int_0^t\frac{v\omega L(v,\omega)d\omega\,dv}{\sqrt{\left(x^2-\omega^2\right)\left(t^2-v^2\right)}}\right],\qquad 0<x<a\,, \tag{6.20}$$

where

$\sigma_1(x)=\dfrac{\sigma_0(x)}{\mu_{12}\theta\,p}$,

$F_1(s,p)=\dfrac{F(s,p)}{s\theta}-1\to 0\ as\ S\to\infty$,

$\theta=\dfrac{\left(C_{12}-C_{22}N_1\alpha_1^{'}\right)\left(\alpha_2^{'}+N_2\right)-\left(C_{12}-C_{22}N_2\alpha_2^{'}\right)\left(\alpha_1^{'}+N_1\right)}{\left(-\alpha_2^{'}N_1+\alpha_1^{'}N_2\right)}$,

$\alpha_j^{'}=\dfrac{C_{11}-N_j^2}{(1+C_{12})N_j}$, $\quad j=1,2$,

$N_{1,2}^2=\dfrac{1}{2C_{22}}\left[C_{11}C_{22}-C_{12}^2+2C_{12}\pm\sqrt{\left(C_{11}C_{22}-C_{12}^2+2C_{12}\right)^2-4C_{11}C_{22}}\right]$

and $L(v,\omega)=\int_0^\infty s\,F_1(s,p)\,J_0(s\omega)\,J_0(sv)ds\,,$ (6.21)

where $J_0(.)$ is the Bessel function of order zero and applying a contour integration technique (Baksi et al. (2003)), the integral in $L(v,\omega)$ can be converted to the following finite integral

$$L(v,\omega)=-\frac{2}{\pi}\frac{p^2}{C_s^2}\left[\int_0^{1/\sqrt{C_{11}}}[A]I_0\left(\frac{p\eta v}{C_s}\right)K_0\left(\frac{p\eta\omega}{C_s}\right)d\eta+\int_{1/\sqrt{C_{11}}}^{0}[C]I_0\left(\frac{p\eta v}{C_s}\right)K_0\left(\frac{p\eta\omega}{C_s}\right)d\eta\right],\ \omega>v, \qquad (6.22)$$

where the expressions [A] and [C] are given in the **Appendix B.**

The corresponding expression of $L(v,\omega)$for $\omega<v$ is obtained by interchanging $v$ and $\omega$ in equation (6.22). Using the asymptotic expression of $I_0(z)$ and $K_0(z)$ as

$I_0(z)\approx 1,$

$K_0(z)\approx \log(2/z).$

Equation (6.22) is reduced to

$$L(v,\omega)=\frac{2}{\pi}P\frac{p^2}{C_s^2}\log\left(\frac{p}{C_s}\right)+O\left(\frac{p^2}{C_s^2}\right), \qquad (6.23)$$

where $P=\frac{1}{\theta}\left[\int_0^{1/\sqrt{C_{11}}}[A]\,d\eta+\int_{1/\sqrt{C_{11}}}^{0}[C]\,d\eta\right].$

Now expressing $f(t)$ as

$$f(t,p)=f_0(t,p)+\frac{p^2}{C_s^2}\log\left(\frac{p}{C_s}\right)f_1(t,p)+O\left(\frac{p^2}{C_s^2}\right),$$

and substituting in equation (6.20), we obtain following equations

$$\frac{d}{dx}\int_0^a f_0(t,p)\log\left|\frac{t+x}{t-x}\right|dt=2\sigma_1(x), \qquad 0\le x<a\ , \qquad (6.24)$$

$$\frac{d}{dx}\int_0^a f_1(t,p)\log\left|\frac{t+x}{t-x}\right|dt=-\frac{4P}{\pi}\int_0^a t\ f_0(t,p)dt, \qquad 0\le x<a.. \qquad (6.25)$$

Now for concentrated loading condition, taking $\sigma(x) = \delta(x - x_0)$, equations (6.24) and (6.25) with the help of Cooke's result (1970) yields unknown function $f(t, p)$ as

$$f(t,p) = \frac{4}{\pi^2 \mu_{12} \theta\, p} \frac{t\sqrt{a^2 - x_0^2}}{\sqrt{a^2 - t^2}} \left( \frac{1}{(x_0^2 - t^2)} + \frac{2P}{\pi} \frac{p^2}{C_s^2} \log\left( \frac{p}{C_s} \right) \right) + o\left( \frac{p^2}{C_s^2} \right). \tag{6.26}$$

The stress intensity factor in the *p*-plane is defined as

$$K_I^*(x_0, p) = \lim_{x \to a^+} \sqrt{2(x-a)}\, \sigma_{yy}^*(x, 0). \tag{6.27}$$

Using the inverse Laplace transform, the dynamic stress intensity factor $K_I(t)$ is obtained as

$$\frac{K_I(t)}{K_I(\infty)} = \frac{1}{2\pi i} \int_{Br} \left[ 1 - \frac{2P}{\pi} \frac{p^2}{C_s^2} \log\left( \frac{p}{C_s} \right) \sqrt{a^2 - x_0^2} \right] \frac{e^{pt}}{p} dp, \tag{6.28}$$

where

$$K_I(\infty) = \lim_{t \to \infty} K_I(t) = \lim_{p \to 0} p\, K_I^*(x_0, p). \tag{6.29}$$

The crack opening displacement (COD) in the transformed domain is given by

$$\Delta v(x,0,p) = 2 \int_x^a f(t,p)\, dt, \qquad 0 \le x \le a$$

$$= \frac{8\sqrt{a^2 - x_0^2}}{\pi^2 \mu_{12} \theta\, p} \int_x^a \left[ 1 + \frac{2P}{\pi} \frac{p^2}{C_s^2} \log\left( \frac{p}{C_s} \right) \right] \frac{t\, dt}{(x_0^2 - t^2)\sqrt{a^2 - t^2}}$$

$$= -\frac{8\, Arc\tanh\left( \frac{\sqrt{a^2 - x^2}}{\sqrt{a^2 - x_0^2}} \right)}{\pi^2 \mu_{12} \theta\, p} \left[ 1 + \frac{2P}{\pi} \frac{p^2}{C_s^2} \log\left( \frac{p}{C_s} \right) \right], \qquad 0 \le x \le a\,.$$

Finally the expression of COD in the time domain is obtained as

$$\Delta v(x,0,t) = -\frac{8\,Arc\tanh\left(\frac{\sqrt{a^2-x^2}}{\sqrt{a^2-x_0^2}}\right)}{\pi^2 \mu_{12}\theta\, p}\frac{1}{2\pi i}\int_{Br}\left[1+\frac{P a^2}{\pi}\frac{p^2}{C_s^2}\log\left(\frac{p}{C_s}\right)\right]\frac{e^{pt}}{p}dp\,. \tag{6.30}$$

### 6.4 Results and discussion

In this section numerical calculations of normalized SIFs $K_1(t)/K_1(\infty)$ and crack opening displacement $\Delta v(x,0,t)$ are carried out at different concentrated loading located at different points on the crack surface using an efficient numerical inversion method for Laplace transform proposed by Bellman et al. (1966). The numerical computations are done for two different orthotropic materials viz., graphite-epoxy and glass-epoxy, and the results are described through graphs against the large normalized time variable $C_s\, t/a$ for different particular cases.

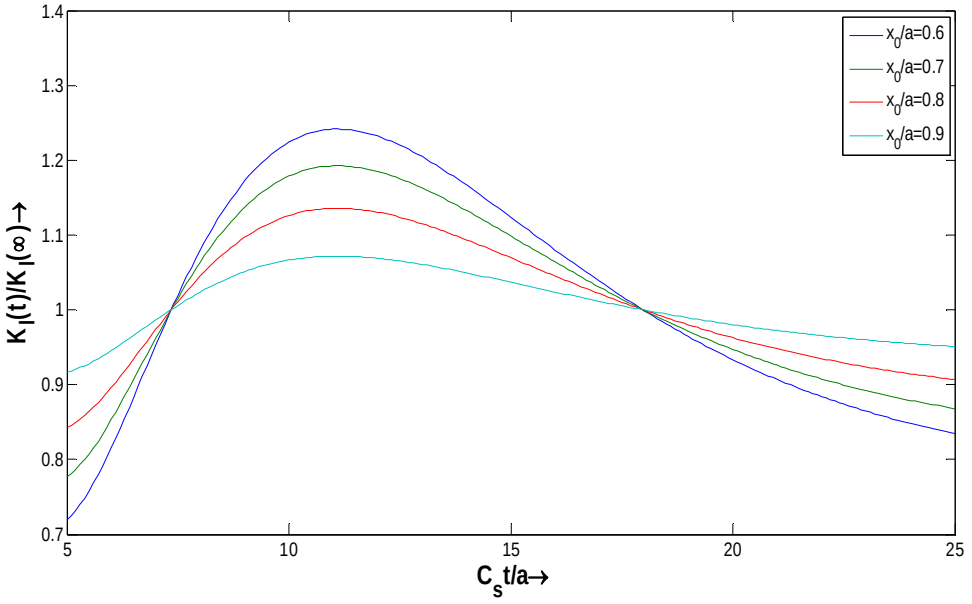


**Fig. 6.1** Plots of $K_I(t)/K_I(\infty)$ against $C_s\, t/a$ for various $x_0/a$ at $h=2$ for graphite epoxy

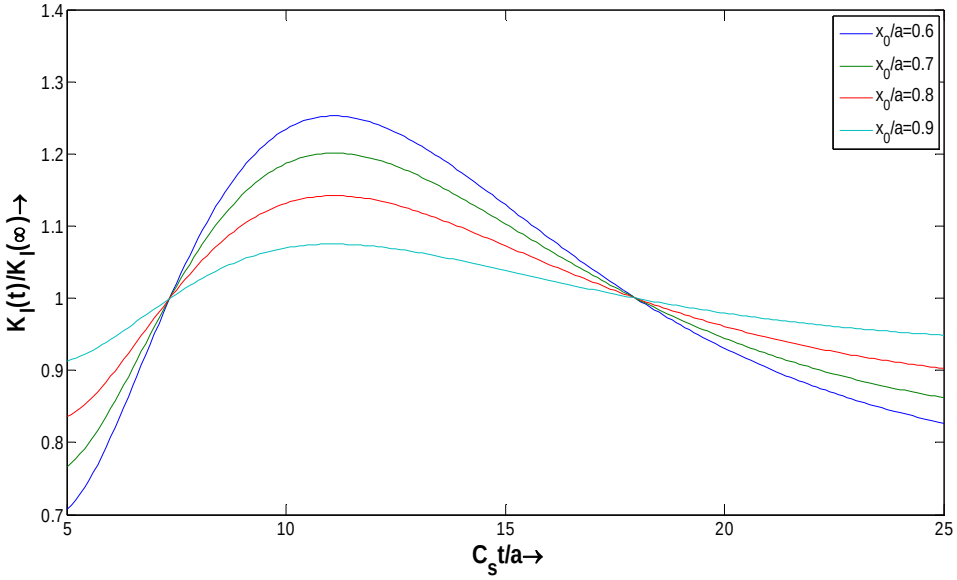


**Fig. 6.2** Plots of $K_I(t)/K_I(\infty)$ against $C_s t/a$ for various $x_0/a$ at $h=4$ for graphite epoxy

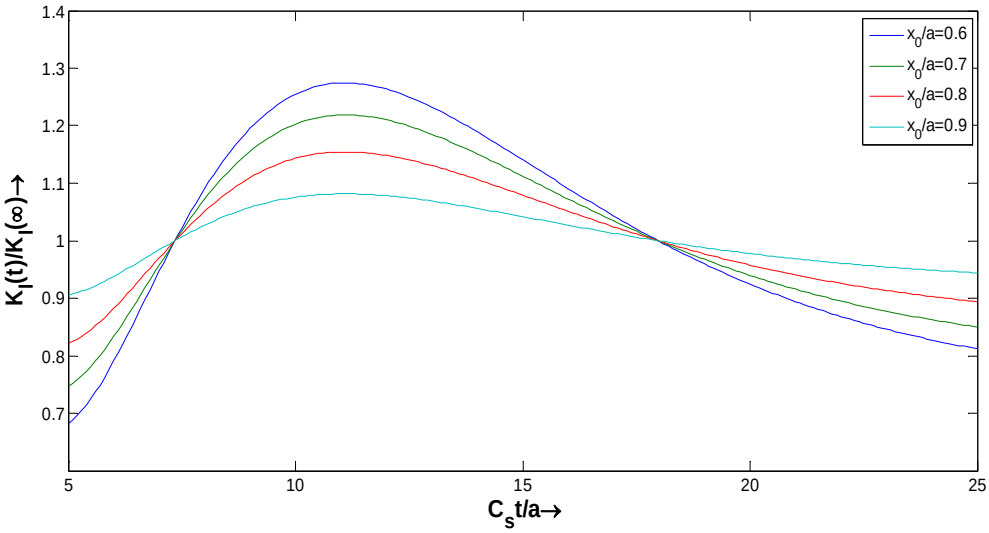


**Fig. 6.3** Plots of $K_I(t)/K_I(\infty)$ against $C_s t/a$ for various $x_0/a$ at $h=6$ for graphite epoxy

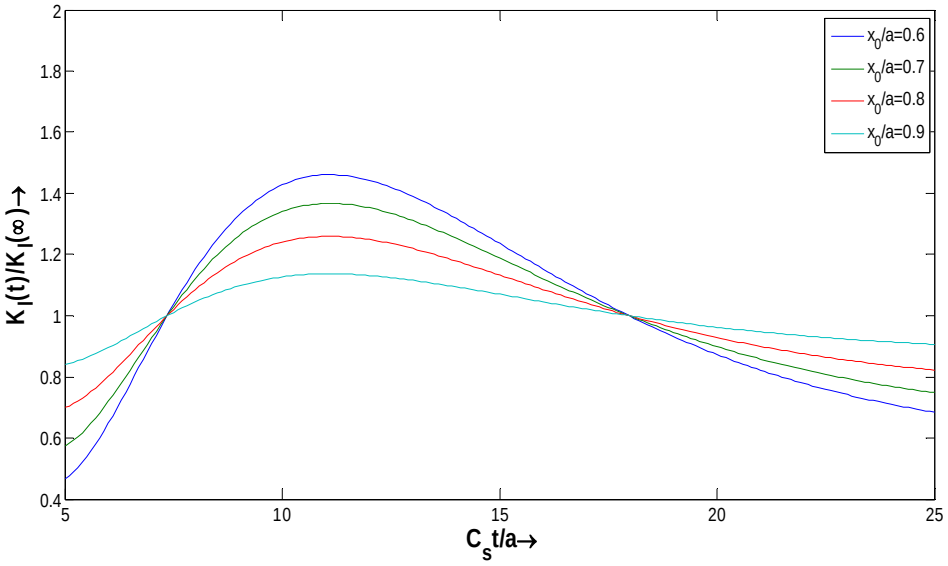


**Fig. 6.4** Plots of $K_I(t)/K_I(\infty)$ against $C_s t/a$ for various $x_0/a$ at $h=2$ for glass-epoxy

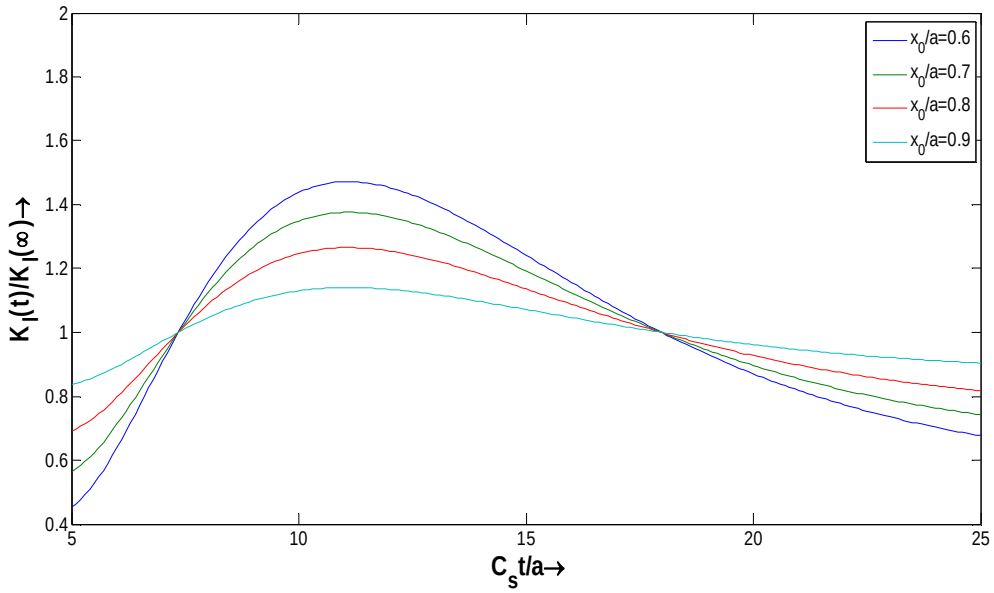


**Fig. 6.5** Plots of $K_I(t)/K_I(\infty)$ against $C_s t/a$ for various $x_0/a$ at $h=4$ for glass-epoxy

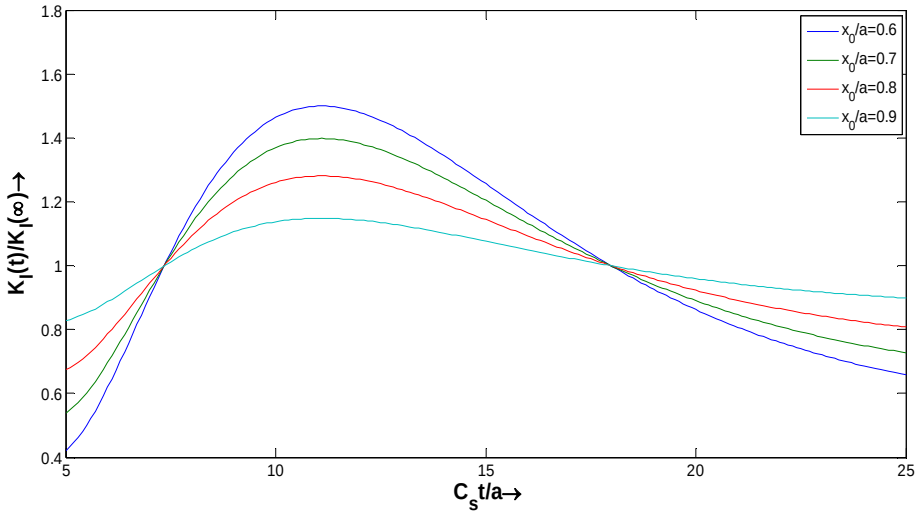


**Fig. 6.6** Plots of $K_I(t)/K_I(\infty)$ against $C_s t/a$ for various $x_0/a$ at $h=6$ for glass-epoxy

During the numerical computation the material constants for the graphite-epoxy composite (type-I) are taken as $E_1=15.3Gpa$, $E_2=158\,Gpa$, $\mu_{12}=5.52\,Gpa$, $\nu_{12}=0.033$ and the material constants for glass-epoxy (type-II) composite are taken as $E_1=9.79\,Gpa$, $E_2=42.3Gpa$, $\mu_{12}=3.66\,Gpa$, $\nu_{12}=0.063$. It is seen from Figs. 6.1-6.6 that initially $K_I(t)/K_I(\infty)$ increases with the increase of $x_0/a=0.6(0.1)0.9$ but when the value $C_s t/a$ close to 7.5, it decreases with the increase of $x_0/a$ for both materials. A close examination of these results reveal that for fixed values of $x_0/a$ and $h$, and for the normalized time $t\le\dfrac{c_s(1+x_0)}{c_d(1-x_0)}$, the dilatation wave does not reach at the crack tip $x=a$ generated from $x=-(x_{0/}/a)$. Some oscillation phenomena are observed which are caused due to arrival of the stress waves and combined effect of Rayleigh and dilatation waves appreciable changes. As a result the normalized dynamic stress intensity factors $K_I(t)/K_I(\infty)$ rise quickly with normalized time greater than or equal to 5, reaching a peak value in the neighbourhood of $C_s t/a=11$ and then decrease in magnitude and finally after a large time it tends to the static solution just like the case of isotropic

material as given by Sih (1991). This behaviour can be attributed to the scattered Rayleigh wave at the crack tip. However, if $x_0 / a \to 1$ then numerical difficulties arise in the solution due to the discontinuity in $K_I^*(x, p)$ at $x_0 / a = 1$. Maximum values of $K_I(t)/K_I(\infty)$ increase with the increase in the values of *h* and almost no time delay is observed between each maximum. When depth of the material becomes large, the normalized stress intensity factors tend to unity for large time. This result agrees with the result given by Kassir and Bandyopadhyay (1983).

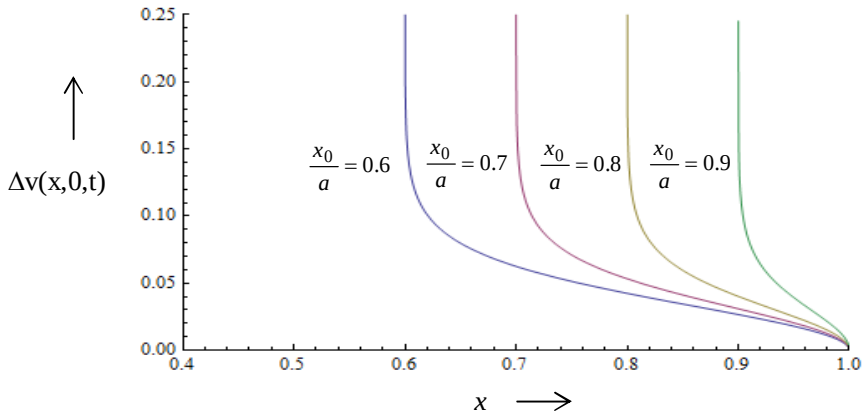


**Fig. 6.7** plots of displacement against field co-ordinate *x* for different values of $x_0 / a$ for graphite-epoxy orthotropic materials

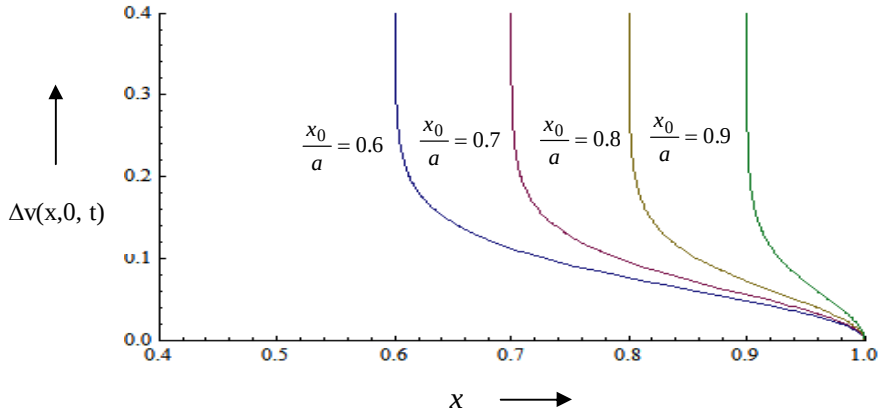


**Fig. 6.8** plots of displacement against field co-ordinate *x* for different values of $x_0 / a$ for glass-epoxy orthotropic materials

It is seen from Figs. 6.7 - 6.8 that the nature of variations of crack opening displacement

is similar with the variation of $x$ for various values of the concentrated loading for both the considered orthotropic materials. The crack opening displacement for both the materials is very small initially near the crack tip due to reason that dilatation waves have little effect on Mode-I stress intensity factor but afterwards it attains large value due to combined effect of elastic waves for different concentrated point loading.

The ratio of the Rayleigh wave speed to the shear wave speed $c_R / c_s$ determines most of the behaviors of $K_I(t)/K_I(\infty)$ including the time of the singularities and jumps. This explains why the plots in Figs. 6.4 - 6.8 are so similar even though they correspond to different materials. Each one has a very similar $c_R / c_s$ ratio. In fact this ratio does not change dramatically for a wide range of materials.

Since the above analysis is valid for large normalized time, the oscillations of the normalized dynamic stress intensity factor during $C_s t / a < 5$ have not been studied. However, the reaching of peak values of $K_I(t)/K_I(\infty)$ has been noticed in our analysis. These situations are predominantly caused by the interaction of waves emanating from the crack-tip.

**6.5 Conclusion**

In this chapter the major contribution is finding the analytical expressions of the dynamic stress intensity factor and crack tip opening displacement of a crack embedded in an orthotropic elastic strip under normal impact concentration loading. The presentation of the singularities occurred in the form of oscillations arising due to arrival of the stress waves generated at crack tips $x = \pm(x_0 / a)$ is another contribution of the study. The most important part of the study is the successful implementation of the efficient and powerful numerical technique used to find the numerical inversion of Laplace transform towards finding the solution in time domain.

# Appendix-A

**Bellman method**

The Laplace transform of a function $f(t)$ is defined by

$$\overline{F}(p)=\int_0^{\infty} f(t)e^{-pt}\,dt, \quad p>0. \tag{A1}$$

We assume that $f(t)$ is sufficiently smooth to permit the approximate method we apply.

Putting $x=e^{-t}$ in equation (A1) we obtain

$$\overline{F}(p)=\int_0^1 x^{p-1}C(x)dx, \tag{A2}$$

where $C(x)=f(-\ln(x))$.

Applying the Gaussian quadrature formula to equation (A2) yields

$$\sum_{i=1}^{N} W_i x_i^{p-1} C(x_i)=\overline{F}(p), \tag{A3}$$

where $x_i\,(i=1,2,...N)$ are the roots of the shifted Legendre polynomial $P_N(x)=0$ and

$W_i\,(i=1,...N)$ are corresponding weights

$$W_1x_1^{p-1}C(x_1)+W_2x_2^{p-1}C(x_2)+W_3x_3^{p-1}C(x_3)+...+W_Nx_N^{p-1}C(x_N)=\overline{F}(p).$$

Put $p=1,...,N$ equation (A3) yields

$$\left.\begin{aligned}
&W_1C(x_1)+W_2C(x_2)+W_3C(x_3)+...+W_NC(x_N)=\overline{F}(1)\\
&W_1x_1\,C(x_1)+W_2x_2\,C(x_2)+W_3x_3\,C(x_3)+...+W_Nx_4\,C(x_N)=\overline{F}(2)\\
&\cdots\cdots\cdots\cdots\cdots\cdots\cdots\cdots\cdots\cdots\cdots\cdots\cdots\cdots\cdots\cdots\cdots\cdots\cdots\cdots\cdots\cdots\\
&W_1x_1^{N-1}C(x_1)+W_2x_2^{N-1}C(x_2)+W_3x_3^{N-1}C(x_3)+...+W_Nx_N^{N-1}C(x_N)=\overline{F}(N)
\end{aligned}\right\}. \tag{A4}$$

Matrix form of system of equation (A4)

$$\begin{bmatrix} W_1 & W_2 \ldots\ldots\ldots\ldots W_N \\ W_1 x_1 & W_2 x_2 \ldots\ldots\ldots\ldots W_N x_N \\ . & \\ . & \\ . & \\ W_1 x_1^{N-1} & W_2 x_2^{N-1} \quad W_N x_N^{N-1} \end{bmatrix} \begin{bmatrix} C(x_1) \\ C(x_2) \\ . \\ . \\ . \\ C(x_N) \end{bmatrix} = \begin{bmatrix} \overline{F}(1) \\ \overline{F}(2) \\ . \\ . \\ . \\ \overline{F}(N) \end{bmatrix}. \tag{A5}$$

The discrete values of $C(x_i)$ are calculated from equation (A5), i.e., $f(t_i)$ and finally the function $f(t)$ can be calculated using interpolation.

## Appendix-B

$$[A] = -\frac{\left(C_{12}\eta^2 - C_{22}\overline{\alpha_1}\,\overline{\gamma_1}\right)\overline{\delta_1}(S) + \left(C_{12}\eta^2 - C_{22}\overline{\alpha_2}\,\overline{\gamma_2}\right)\overline{\delta_2}(S)}{\theta\left(\overline{\alpha_1} - \overline{\beta}\,\overline{\alpha_2}\right)}$$

$$[C] = \frac{\hat{\beta}\left(C_{12}\eta^2 - C_{22}\,\hat{\alpha}_2\,\hat{\gamma}_2\right)}{\theta\left(\hat{\alpha}_1 + \hat{\beta}\,\hat{\alpha}_2\right)} - \frac{2\left(C_{12}\eta^2 - C_{22}\,\hat{\alpha}_2\,\hat{\gamma}_2\right)\left\{\left(\hat{\alpha}_1^{\,2} - \hat{\alpha}_2^{\,2}\right)\sin 2\hat{\gamma}_1 h - 2\hat{\alpha}_1\hat{\alpha}_2\cos 2\hat{\gamma}_1 h\right\}}{\theta\left(\hat{\alpha}_1^{\,2} + \hat{\alpha}_2^{\,2}\right)\left(\hat{\alpha}_1 + \hat{\beta}\hat{\alpha}_2\right)}$$

$$\overline{\delta_1}(S) = \frac{\overline{\alpha_2}\,\overline{\beta} + \overline{\alpha_2}\,sh\overline{\gamma_1}h\,sh\overline{\gamma_2}h - \overline{\alpha_1}\,ch\overline{\gamma_1}h\,ch\overline{\gamma_2}h}{\overline{\alpha_1}\,ch\overline{\gamma_1}h\,ch\overline{\gamma_2}h - \overline{\alpha_1}\,sh\overline{\gamma_1}h\,sh\overline{\gamma_2}h},$$

$$\overline{\delta_2}(S) = \frac{\overline{\alpha_1} + \overline{\alpha_1}\,\overline{\beta}\,sh\overline{\gamma_1}h\,ch\overline{\gamma_2}h - \overline{\alpha_2}\,\overline{\beta}\,ch\overline{\gamma_1}h\,sh\overline{\gamma_2}h}{\overline{\alpha_1}\,ch\overline{\gamma_1}h\,ch\overline{\gamma_2}h - \overline{\alpha_2}\,sh\overline{\gamma_1}h\,sh\overline{\gamma_2}h},$$

$$\overline{\gamma_1} = \left[\frac{1}{2}\left\{B_1 + \sqrt{B_1^2 - 4B_2}\right\}\right]^{1/2}, \overline{\gamma_2} = \left[\frac{1}{2}\left\{B_1 - \sqrt{B_1^2 - 4B_2}\right\}\right]^{1/2},$$

$$\hat{\gamma_1} = \left[\frac{1}{2}\left\{B_1 + \sqrt{B_1^2 - 4B_2}\right\}\right]^{1/2}, \hat{\gamma_2} = \left[\frac{1}{2}\left\{-B_1 - \sqrt{B_1^2 - 4B_2}\right\}\right]^{1/2},$$

$$B_1 = \frac{1}{C_{22}}\left[\left(C_{12}^2 + 2C_{12} - C_{11}C_{22}\right)\eta^2 + \left(1 + C_{22}\right)\right],\ B_2 = \frac{1}{C_{22}}\left(\frac{1}{C_{11}} - \eta^2\right)\left(1 - \eta^2\right).$$

$$\overline{\alpha_i} = \frac{C_{11}\eta^2 - 1 + \overline{\gamma_i}^2}{(1 + C_{12})\overline{\gamma_i}}, \quad \hat{\alpha}_i = \frac{C_{11}\eta^2 - 1 + (-1)^i \hat{\gamma}_i^2}{(1 + C_{12})\hat{\gamma}_i}, \; i = 1,2.$$

$$\overline{\beta} = \frac{\overline{\gamma_1} - \overline{\alpha_1}}{\overline{\gamma_2} - \overline{\alpha_2}}, \; \hat{\beta} = \frac{\hat{\gamma}_1 + \hat{\alpha}_1}{\hat{\gamma}_2 - \hat{\alpha}_2}.$$